J|A|C|S
ARTICLES
Published on Web 12/08/2006

Two-Dimensional Porous Molecular Networks of Dehydrobenzo[12]annulene Derivatives via Alkyl Chain Interdigitation

Kazukuni Tahara,[†] Shuhei Furukawa,[‡] Hiroshi Uji-i,[‡] Tsutomu Uchino,[†] Tomoyuki Ichikawa,[†] Jian Zhang,[‡] Wael Mamdouh,[‡] Motohiro Sonoda,[†] Frans C. De Schryver,[‡] Steven De Feyter,*[,‡] and Yoshito Tobe*[,†]

Contribution from the Division of Frontier Materials Science, Graduate School of Engineering Science, Osaka University, Toyonaka, Osaka 560-8531, Japan, and Department of Chemistry, Division of Molecular and Nanomaterials, Laboratory of Photochemistry and Spectroscopy, and Institute of Nanoscale Physics and Chemistry, Katholieke Universiteit Leuven (KULeuven), Celestijnenlaan 200 F, B-3001 Leuven, Belgium

Received August 1, 2006; E-mail: Steven.DeFeyter@chem.kuleuven.be; tobe@chem.es.osaka-u.ac.jp.

Abstract: The self-assembly of a series of hexadehydrotribenzo[12]annulene (DBA) derivatives has been scrutinized by scanning tunneling microscopy (STM) at the liquid−solid interface. First, the influence of core symmetry on the network structure was investigated by comparing the two-dimensional (2D) ordering of rhombic bisDBA **1a** and triangular DBA **2a** (Figure 1). BisDBA **1a** forms a Kagomé network upon physisorption from 1,2,4-trichlorobenzene (TCB) onto highly oriented pyrolytic graphite (HOPG). Under similar experimental conditions, DBA **2a** shows the formation of a honeycomb network. The core symmetry and location of alkyl substituents determine the network structure. The most remarkable feature of the DBA networks is the interdigitation of the nonpolar alkyl chains: they connect the π-conjugated cores and direct their orientation. As a result, 2D open networks with voids are formed. Second, the effect of alkyl chain length on the structure of DBA patterns was investigated. Upon increasing the length of the alkyl chains (DBAs **3c**−**e**) a transition from honeycomb networks to linear networks was observed in TCB, an observation attributed to stronger molecule−substrate interactions. Third, the effect of solvent on the structure of the nonpolar DBA networks was investigated in four different solvents: TCB as a polar aromatic solvent, 1-phenyloctane as a solvent having both aromatic and aliphatic moieties, *n*-tetradecane as an aliphatic solvent, and octanoic acid as a polar alkylated solvent. The solvent dramatically changes the structure of the DBA networks. The solvent effects are discussed in terms of factors that influence the mobility of molecules at the liquid−solid interface such as solvation.

Introduction

The control of the spatial organization of functional π-electron-conjugated systems[1] has led to major advances in the field of organic materials, such as liquid crystal materials, molecular-scale electronics,[2] and molecular devices.[3] Recently, the structural control of organic monolayers has been presented as a further important step to achieve highly ordered organic nanostructures and also as an opportunity to fabricate molecular scale devices on flat substrates.[1b,4] Scanning tunneling microscopy (STM) is a powerful technique for the investigation of two-dimensional (2D) crystal structures of π-electron-conjugated systems with atomic scale resolution. STM not only operates under ultrahigh vacuum conditions but also at the interface between two condensed media; one is an atomically flat conducting solid and the other is a gas, a liquid, a liquid crystalline material, or a gel.

One of the useful approaches is to decorate the surface with molecules that form regular 2D periodic patterns by self-assembly at the liquid−solid interface.[5] In such systems, it is essential to control the competition between the following four modes of interaction to construct the desired molecular patterns; molecule−molecule, molecule−substrate, molecule-solvent, and solvent−substrate interactions. Especially, the control of mol-

[†] Osaka University.
[‡] Katholieke Universiteit Leuven.

(1) (a) Hoeben, F. J. M.; Jonkheijm, P.; Meijer, E. W.; Schenning, A. P. H. J. *Chem. Rev.* **2005**, *105*, 1491−1546. (b) Grimsdale, A. C.; Müllen, K. *Angew. Chem., Int. Ed.* **2005**, *44*, 5592−5629.
(2) (a) Joachim, C.; Gimzewski, J. K.; Aviram, A. *Nature* **2000**, *408*, 541−548. (b) Nitzan, A.; Ratner, M. A. *Science* **2003**, *300*, 1384−1389.
(3) Collier, C. P.; Mattersteig, G.; Wong, E. W.; Luo, Y.; Beverly, K.; Sampaio, J.; Raymo, F. M.; Stoddart, J. F.; Heath, J. R. *Science* **2000**, *289*, 1172−1175.
(4) (a) Samorí, P.; Severin, N.; Simpson, C. D.; Müllen, K.; Rabe, J. P. *J. Am. Chem. Soc.* **2002**, *124*, 9454−9457. (b) Piot, L.; Marchenko, A.; Wu, J.; Müllen, K.; Fichou, D. *J. Am. Chem. Soc.* **2005**, *127*, 16245−16250. (c) Okawa, Y.; Aono, M. *Nature* **2001**, *409*, 683−684.
(5) For recent reviews on STM measurements at the liquid−solid interface, see, for example: (a) De Feyter, S.; De Schryver, F. C. *Chem. Soc. Rev.* **2003**, *32*, 139−150. (b) De Feyter, S.; De Schryver, F. C. *J. Phys. Chem. B* **2005**, *109*, 4290−4302. (c) Samorí, P.; Rabe, J. P. *J. Phys.: Condens. Matter* **2002**, *14*, 9955−9973. (d) Giancarlo, L. C.; Flynn, G. W. *Acc. Chem. Res.* **2000**, *33*, 491−501. (e) Wan, L.-J. *Acc. Chem. Res.* **2006**, *39*, 334−342. (f) Hermann, B. A.; Scherer, L. J; Housecroft, C. E.; Constable, E. C. *Adv. Funct. Mater.* **2006**, *16*, 221−235.

10.1021/ja0655441 CCC: $33.50

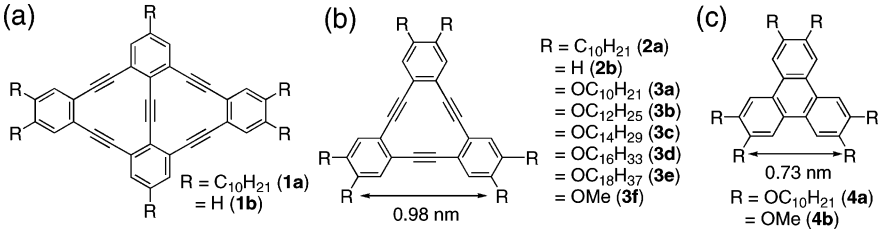

Figure 1. Structures of (a) decadehydrotetrabenzo[12]annuleno[12]annulene (bisDBAs, **1a**,**b**), (b) hexadehydrotribenzo[12]annulene (DBA, **2a**−**b** and **3a**−**f**), and (c) triphenylene (**4a**,**b**) derivatives.

ecule−molecule interactions is crucial for the formation of molecular networks: typically, discrete molecular building-blocks are 'connected' to each other by virtue of directional intermolecular interactions such as hydrogen bonding or metal coordination. Being able to correlate molecular features such as shape, position of interacting sites, as well as electronic properties with the resulting topology of the molecular architectures would enable us to design and construct the network structures and their functions. This strategy is already well-known as "crystal engineering" in three-dimensional (3D) crystal systems.[6] Of special interest are 2D molecular porous networks.[7,8]

In 2D systems, the molecule−substrate interaction is an important issue to regulate network topologies in terms of symmetry matching of the molecules with the substrate. The strength of the molecule−substrate interactions can be controlled by adjusting the van der Waals interaction between molecules and substrate. For example, the molecule−substrate interaction on graphite linearly increases with the length of the alkyl chains.[9,10]

At the liquid−solid interface, solvent molecules play a significant role in the network formation and have therefore a strong effect on the network structures. Sometimes solvent molecules are coadsorbed in the molecular network (solvent−substrate interaction).[11] Coadsorption of solvent molecules critically depends among other factors on the size and shape of the solvent molecules[12] as well as the mode of interaction (e.g., hydrogen bonding, van der Waals interactions) between the solvent and the other molecules.[13] The solvent also affects the mobility of the molecules[14] at the liquid−solid interface, e.g., by affecting the adsorption−desorption dynamics. In this dynamic process, the mobility of the molecules is affected by the solvation energy (molecule−solvent interaction) and possibly also by solvent viscosity.[15] Hence, for a successful rational construction of 2D molecular networks, an accurate molecular design taking into account these four interactions is essential.

In this contribution, we systematically study the formation of 2D molecular networks of dehydrobenzo[12]annulene (DBA) derivatives on highly oriented pyrolytic graphite (HOPG). Our strategy to form 2D regular networks is based on choosing rigid π-electron-conjugated frameworks with long alkyl chains as molecular building-blocks. In this respect, DBA derivatives are good candidates because of their planar π-electron-conjugated framework, unique molecular shape, suitable core size to favor directional alkyl chain interdigitation, and core symmetry which fits the graphite lattice (Figure 1).[16] Furthermore, their synthetic versatility allows chemical modification of their periphery.[17]

Instead of using hydrogen bonds,[5,7,18] we focus on directional alkyl chain interdigitation and tune the strength of molecule−molecule and molecule−substrate interactions by stepwise elongation of the alkyl chains. For that purpose, in addition to the previously synthesized decyl-substituted rhombic-shaped bisDBA **1a** and triangular-shaped DBA **2a**, a series of DBA derivatives with alkoxy chains of variable length **3a**−**e** were synthesized (Figure 1).

(6) (a) Schmidt, G. M. J. *Pure Appl. Chem.* **1971**, *27*, 647−678. (b) *Crystal Engeering: The Design of Organic Solid*; Desiraju, G. R., Ed.; Elsevier: New York, 1989. (c) Desiraju, G. R. *Angew. Chem., Int. Ed. Engl.* **1995**, *34*, 2311−2327. (d) Blagden, N.; Davey, R. J. *Cryst. Growth Des.* **2003**, *3*, 873−885.
(7) (a) Theobald, J. A.; Oxtoby, N. S.; Phillips, M. A.; Champness, N. R.; Beton, P. H. *Nature* **2003**, *424*, 1029−1031. (b) Stepanow, S.; Lingenfelder, M.; Dmitriev, A.; Spillmann, H.; Delvigne, E.; Lin, N.; Deng, X.; Cai, C.; Barth, J. V.; Kern, K. *Nature Mat.* **2004**, *3*, 229−233. (c) Li, Z.; Han, B.; Wan, L. J.; Wandlowski, Th. *Langmuir* **2005**, *21*, 6915−6928. (d) Ishikawa, Y.; Ohira, A.; Sakata, M.; Hirayama, C.; Kunitake, M. *Chem. Commun.* **2002**, 2652−2653. (e) Lu, J.; Lei, S. B.; Zeng, Q. D.; Kang, S. Z., Wang, C.; Wan, L. J.; Bai, C. L. *J. Phys. Chem. B* **2004**, *108*, 5161−5165. (f) Griessl, S. J. H.; Lackinger, M.; Jamitzky, F.; Markert, T.; Hietschold, M.; Heckl, W. M. *J. Phys. Chem. B* **2004**, *108*, 11556−11560. (g) Griessl, S. J. H.; Lackinger, M.; Jamitzky, F.; Markert, T.; Hietschold, M.; Heckl, W. M. *Langmuir* **2004**, *20*, 9403−9407.
(8) (a) Liu, Y.; Lei, S.; Yin, S.; Xu, S.; Zheng, Q.; Zeng, Q.; Wang, C.; Wan, L.; Bai, C. *J. Phys. Chem. B* **2002**, *106*, 12569−12574. (b) Gyarfas, B. J.; Wiggins, B.; Zosel, M.; Hipps, K. W. *Langmuir* **2005**, *21*, 919−923. (c) Jeong, K. S.; Kim, S. Y.; Shin, U. S.; Kogej, M; Hai, N. T. M.; Broekmann, P.; Jeong, N; Kirchner, B.; Reiher, M.; Schalley, C. A. *J. Am. Chem. Soc.* **2005**, *127*, 17672−17685. (d) Schull, G.; Douillard, L.; Fiorini-Debuisschert, C.; Charra, F.; Mathevet, F.; Kreher, D.; Attias, A.-J. *Nano Lett.* **2006**, *6*, 1360−1363.
(9) (a) Smith, D. P. E.; Hörber, H.; Gerber, C.; Binnig, G. *Science* **1989**, *245*, 43−45. (b) Smith, D. P. E.; Hörber, J. K. H.; Binning, G.; Nejoh, H. *Nature* **1990**, *344*, 641−644. (c) Hara, M.; Iwakabe, Y.; Tochigi, K.; Sasabe, H.; Garito, A. F.; Yamada, A. *Nature* **1990**, *344*, 228−230.
(10) (a) Paserba, K. R.; Gellman, A. J. *J. Chem. Phys.* **2001**, *115*, 6737−6751. (b) Paserba, K. R.; Gellman, A. J. *Phys. Rev. Lett.* **2001**, *86*, 4338−4341. (c) Müller, T.; Flynn, G. W.; Mathauser, A. T.; Teplyakov, A. V. *Langmuir* **2003**, *19*, 2812−2821.
(11) (a) Yablon, D. G.; Wintgens, D.; Flynn, G. W. *J. Phys. Chem. B* **2002**, *106*, 5470−5475. (b) Vanoppen, P.; Grim, P. C. M.; Rücker, M.; De Feyter, S.; Moessner, G.; Valiyaveettil, S.; Müllen, K.; De Schryver, F. C. *J. Phys. Chem.* **1996**, *100*, 19636−19641.
(12) Mamdouh, W.; Uji-i, H.; Ladislaw, J. S.; Dulcey, A. E.; Percec, V.; De Schryver, F. C.; De Feyter, S. *J. Am. Chem. Soc.* **2006**, *128*, 317−325.
(13) Nath, K. G.; Ivasenko, O.; Miwa, J. A.; Dang, H.; Wuest, J. D. Nanci, A.; Perepichka, D. F.; Rosei, F. *J. Am. Chem. Soc.* **2006**, *128*, 4212−4213.
(14) (a) Kim. K.; Plass, K. E.; Matzger, A. J. *Langmuir* **2003**, *19*, 7149−7152. (b) Kim, K.; Plass, K. E.; Matzger, A. J. *J. Am. Chem. Soc.* **2005**, *127*, 4879−4887.
(15) (a) Venkataraman, B.; Breen, J. J.; Flynn, G. W. *J. Phys. Chem.* **1995**, *99*, 6608−6619. (b) Li, C.-J.; Zeng, Q.-D.; Wang, C.; Wan, L.-J.; Xu, S.-L.; Wang, C.-R.; Bai, C.-L. *J. Phys. Chem. B* **2003**, *107*, 747−750. (c) Lackinger, M.; Griessl, S.; Heckl, W. M.; Hietschold, M.; Flynn, G. W. *Langmuir* **2005**, *21*, 4984−4988. (d) Kampschulte, L.; Lackinger, M.; Maier, A.-K.; Kishore, R. S. K.; Griessl, S.; Schmittel, M.; Heckl, W. M. *J. Phys. Chem. B* **2006**, *110*. 10829−10836. (e) Shao, X.; Luo, X.; Hu, X.; Wu. K. *J. Phys. Chem. B* **2006**, *110*, 1288−1293.
(16) Furukawa, S.; Uji-i, H.; Tahara, K.; Ichikawa, T.; Sonoda, M.; De Schryver, F. C.; Tobe, Y.; De Feyter, S. *J. Am. Chem. Soc.* **2006**, *128*, 3502−3503.
(17) Youngs, W. J.; Tessier, C. A.; Bradshaw, J. D. *Chem. Rev.* **1999**, *99*, 3153−3180.
(18) There are a number of papers about 2D molecular network through the hydrogen bonding as connectivity. See, for example: (a) Griessl, S.; Lackinger, M.; Edelwirth, M.; Hietschold, M.; Heckl, W. M. *Single Mol.* **2002**, *3*, 25−31. (b) Lei, S. B.; Wang, C.; Yin, S. X.; Wang, H. N.; Xi, F.; Liu, H. W.; Xu, B.; Wan, L. J.; Bai, C. L. *J. Phys. Chem. B* **2001**, *105*, 10838−10841. (c) Otsuki, J.; Nagamine, E.; Kondo, T.; Iwasaki, K.; Asakawa, M.; Miyake, K. *J. Am. Chem. Soc.* **2005**, *127*, 10400−10405.

Scheme 1. Synthesis of Hexaalkoxy DBA **3a**−**e**

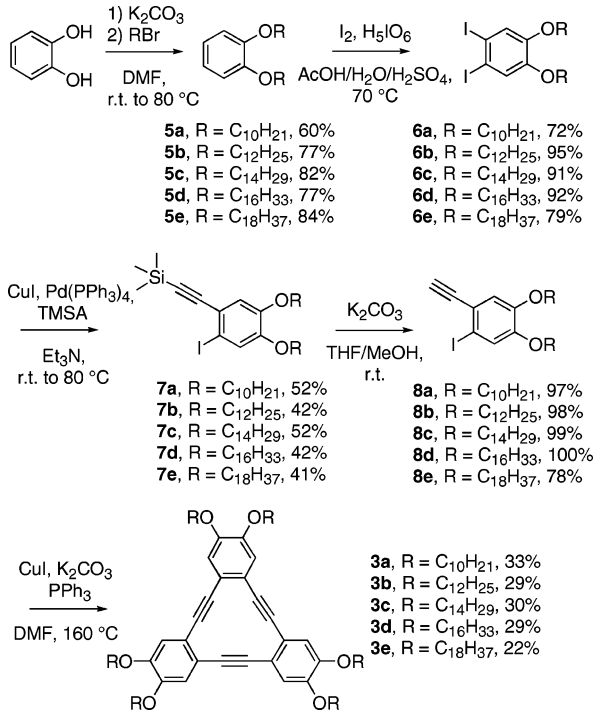

The solvent turned out to be an important factor as the 2D patterns were dramatically affected by the nature of the solvent. Previous studies of solvent effects were mainly focused on 2D molecular networks held together by hydrogen bonding[15a−d] or lamella-type structures of alkylated molecules stabilized by van der Waals interactions.[14,15e] The present investigation highlights the important role of solvent on the structure and stabilization of molecular networks which are formed, not via hydrogen bonding, but via the interaction between nonpolar groups based upon van der Waals interactions, i.e., directional alkyl chain interdigitation.

Results

1. Synthesis. Two sets of DBA derivatives with different core shapes, rhombus and triangle, are selected for the STM investigations. The synthesis of bisDBA **1a** and DBA **2a** having six decyl chains was reported previously.[19] To modify the alkyl chain length of the triangle-shaped DBAs, hexaalkoxy DBAs (**3a**−**e**) (R = $C_{10}H_{21}$; **3a**, $C_{12}H_{25}$; **3b**, $C_{14}H_{29}$; **3c**, $C_{16}H_{33}$; **3d**, $C_{18}H_{37}$; **3e**) were synthesized from catechol. The synthesis of DBAs **3a**−**e** is outlined in Scheme 1. Catechol was alkylated by treatment with the respective alkyl bromide to yield 1,2-dialkoxybenzenes **5a**−**e**. Iodination of **5a**−**e** with periodic acid and iodine in a mixture of acetic acid, water, and H_2SO_4 gave 1,2-dialkoxy-4,5-diiodobenzenes **6a**−**e**.[20,21] Diiodides **6a**−**e** were treated with (trimethylsilyl)acetylene (TMSA) in the presence of copper iodide and $Pd(PPh_3)_4$ as catalysts to give 1,2-dialkoxy-3-iodo-4-(trimethylsilyl)ethynylbenzenes **7a**−**e**. Deprotection of the trimethylsilyl group of the coupling products was performed by stirring with potassium carbonate in methanol/THF (1:1), giving **8a**−**e**. For the construction of the annulene framework, the copper-catalyzed cyclotrimerization of **8a**−**e** was employed.[22] The reaction of **8a**−**e** with copper iodide and triphenylphosphine in DMF proceeded smoothly at 160 °C to afford hexasubstituted DBAs **3a**−**e** in modest yields.[23]

2. STM Observation of DBA Networks at the Liquid−Solid Interface. First, the formation of DBA networks at the 1,2,4-trichlorobenzene (TCB)−graphite interface was probed for **1a**, **2a**, and **3a**−**e** in order to evaluate the effect of the π-electron core symmetry as well as the length of the alkyl chains on the geometry of the 2D networks. In a next step, the spontaneous monolayer formation was repeated in several solvents to elucidate how the choice of solvent affects the structure of the typical DBA networks formed at the TCB−HOPG interface, i.e., the Kagomé lattice of **1a**, the honeycomb structure of **2a** and **3a**, and the linear B array of **3d** (see below). The choice of these solvents was motivated by their different characteristics: TCB as a polar aromatic solvent, 1-phenyloctane as a solvent having both aromatic and aliphatic moieties, *n*-tetradecane as an aliphatic solvent, and 1-octanoic acid as a polar alkylated solvent. All experiments were performed at 20−22 °C.

2.1. Molecular Networks of DBA Derivatives 1a, 2a, and 3a−e in TCB. (a) Structure and Dynamic Behavior of 1a. Figures 2a and 2c display STM images of a physisorbed monolayer obtained from a solution of bisDBA **1a** in TCB on HOPG. In the STM images, aromatic moieties are often observed to show a high tunneling efficiency allowing a straightforward interpretation of the bright−dark contrast in the images.[24] Therefore, bright rhombic features correspond to the π-electron-conjugated cores,[25] which also agrees with the molecular size. The striped features between the π-systems correspond to alkyl chains. Surprisingly, a dynamic change of the molecular alignment of **1a** was observed; early on in a measuring session, a linear network (linear A) was observed (Figure 2a)[26] which was then gradually replaced by a Kagomé domain (Figure 2c). This observation suggests that the linear A structure is a kinetically favored molecular pattern while the Kagomé network is the thermodynamically more stable one.[14a]

A model reflecting the molecular ordering of **1a** according to the linear A type packing is shown in Figure 2b. All molecules are oriented in the same way; extended alkyl chains bridge the gap between adjacent cores. This leads to alkyl chain interdigitation at two sides (2 times two alkyl chains per core) while at the other two sides, only one alkyl chain per core extends to the adjacent core. All alkyl chains are aligned along two of the main symmetry axes of graphite. A unit cell contains one molecule of **1a**, and the cell parameters are $\alpha = 2.4 \pm 0.1$ nm, $\beta = 2.6 \pm 0.1$ nm, and $\gamma = 101 \pm 4°$.

A packing model of the Kagomé network of **1a** is presented in Figure 2d. Again, the interaction between adjacent molecules is based on alkyl chain interdigitation, now at all sides, involving

(19) Sonoda, M.; Sakai, Y.; Yoshimura, T.; Tobe, Y.; Kamada, K. *Chem. Lett.* **2004**, 972−973.
(20) Kovalenko, S. V.; Peabody, S.; Manoharan, M.; Clark, R. J.; Alabugin, I. V. *Org. Lett.* **2004**, *6*, 2457−2460.
(21) Compounds **6a**−**6c** were previously known. (a) Zhang, D.; Tessier, C. A.; Youngs, W. J. *Chem. Mater.* **1999**, *11*, 3050−3057. (b) Zhou, Q.; Carroll, P. J.; Swager, T. M. *J. Org. Chem.* **1994**, *59*, 1294−1301. (c) Ong, C. W.; Liao, S.-C.; Chang, T. H.; Hsu, H.-F. *J. Org. Chem.* **2004**, *69*, 3181−3185.
(22) Iyoda, M.; Sirinintasak, S.; Nishiyama, Y.; Vorasingha, A.; Sultana, F.; Nakao, K.; Kuwatani, Y.; Matsuyama, H.; Yoshida, M.; Miyake, Y. *Synthesis* **2004**, 1527−1531.
(23) Hexaalkoxy[12]DBAs **3a** and **3c** were reported in, ref. 21a.
(24) Lazzaroni, R.; Calderone, A.; Lambin, G.; Rabe, J. P.; Brédas, J. L. *Synth. Met.* **1991**, *41*, 525−528.
(25) The bright features also match the shape of the frontier orbitals of model compound **1b** (see Supporting Information).
(26) The yellow line in Figure 2a indicates the domain boundary that is originated form the difference of the alkyl chains interdigitation pattern.

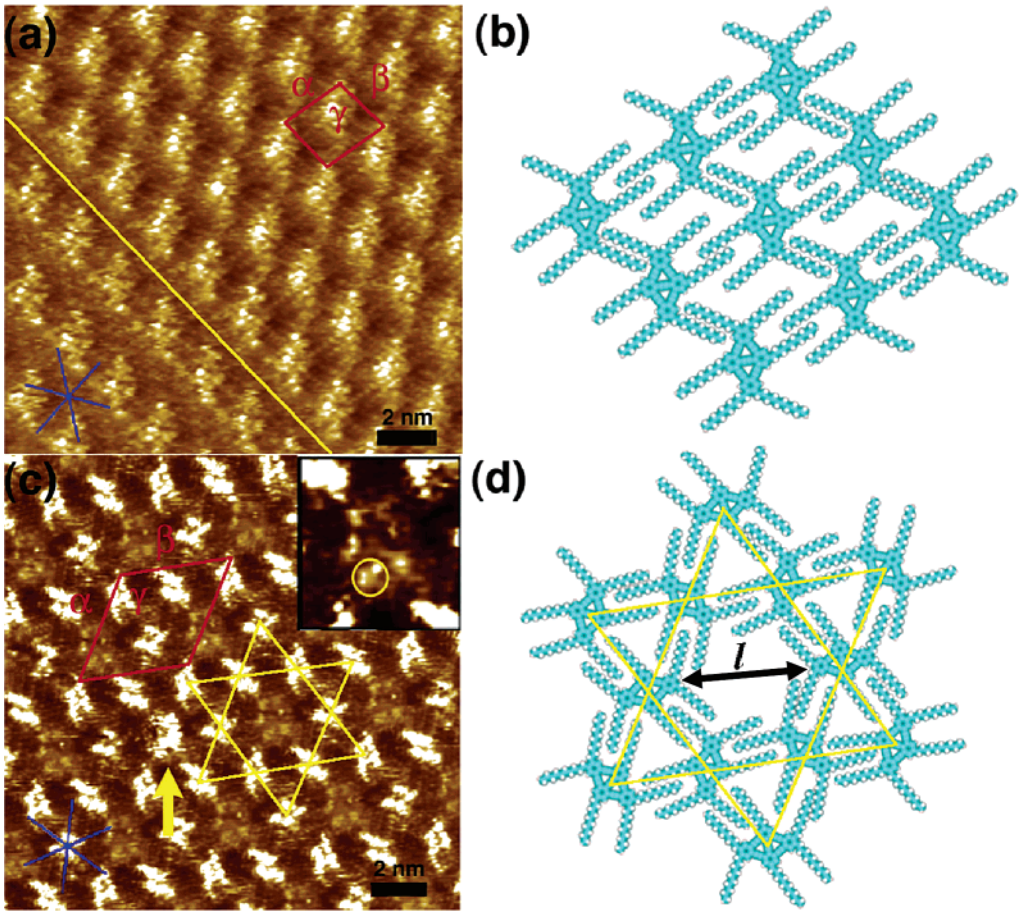

Figure 2. STM images of bisDBA **1a** physisorbed from TCB on HOPG and their model structures. (a) Linear A network of bisDBA **1a** (I_{scl} = 0.50 nA, V_{bias} = −1.04 V). The yellow line indicates a domain boundary. (b) Molecular model of the linear A network of **1a**. (c) The Kagomé network of bisDBA **1a** (I_{scl} = 0.50 nA, V_{bias} = −1.04 V). Inset: Expansion of the central void of the Kagomé structure. The yellow circle in the inset indicates the positions of some bright spots, attributed to TCB molecules. The yellow arrow indicates a trapped bis-annulene molecule in the center of a void. (d) Molecular model of the Kagomé network of **1a**. The main symmetry axes of graphite are indicated in the lower left corner of the STM images.

in total three alkyl chains per side (2 + 1). The alkyl chains run parallel to the main graphite axes underneath. A unit cell contains three molecules of **1a**. The cell parameters of the Kagomé network are $\alpha = 5.0 \pm 0.1$ nm, $\beta = 4.9 \pm 0.1$ nm, and $\gamma = 120 \pm 1°$.

In the Kagomé network, the cyclic arrangement of six molecules leads to the formation of a void. The average diameter of the void estimated from the distance between the π-electron moieties of **1a** having the same orientation across the void is $l = 3.2 \pm 0.2$ nm (Figure 2d). By taking into account the size of the void, it is likely to be filled by six TCB solvent molecules (inset in Figure 2c).[16] In addition, during the measurements, occasionally a fuzzy but bright spot appeared in the center of such a void (yellow arrow in Figure 2c), which we attribute to a trapped bis-annulene molecule. These observations suggest that there is a competition between coadsorption of solvent molecules and **1a** itself in the voids.

(b) Structure of Molecular Network of 2a. Figure 3a presents a typical STM image of a monolayer formed by triangle-shaped compound **2a** upon applying a drop of a solution of **2a** dissolved in TCB onto a freshly cleaved HOPG surface. The bright triangles correspond to the π-conjugated cores of **2a**. A honeycomb network is formed; each apex position of the hexagon is occupied by a molecule of **2a** and the sides of neighboring triangles face each other and are linked by alkyl chain interdigitation (Figure 3b) leading to appreciable intermolecular interactions. Furthermore, the alkyl chains are orientated along the three main symmetry axes of graphite. The cell parameters of the honeycomb network of **2a** are $\alpha = 3.9 \pm 0.1$ nm, $\beta = 3.8 \pm 0.1$ nm, and $\gamma = 119 \pm 1°$. There are two molecules in a unit cell. Again a regular pattern of voids is observed, now as the result of the formation of cyclic hexamers of **2a** as part of the honeycomb network. The average diameter of the void estimated from the distance between π-electron systems of **2a** having the opposite orientation across the void is $l = 3.1 \pm 0.1$ nm (Figure 3b).

(c) Effect of Elongation of the Alkyl Chains of Triangular DBA on the Network Structure. As the length of the alkoxy chains of DBAs **3a**−**e** increases (O−C (terminal) length varies from 1.25 to 2.24 nm), the 2D ordering changes accordingly. DBA **3a** having decyloxy side chains forms a honeycomb network (Figure 4a). The detailed structural features of the honeycomb network of **3a** are similar to those of **2a**. There is no clear difference between the physisorption behavior of compounds **2a** and **3a** in TCB, except for a slight difference in the unit cell parameters: $\alpha = 4.2 \pm 0.1$ nm, $\beta = 3.9 \pm 0.1$ nm, and $\gamma = 122 \pm 1°$ for **3a**; $\alpha = 3.9 \pm 0.1$ nm, $\beta = 3.8 \pm 0.2$ nm, and $\gamma = 119 \pm 1°$ for **2a**.

Figure 4b shows a typical STM image of **3b** at the TCB−graphite interface. The honeycomb structure was dominantly

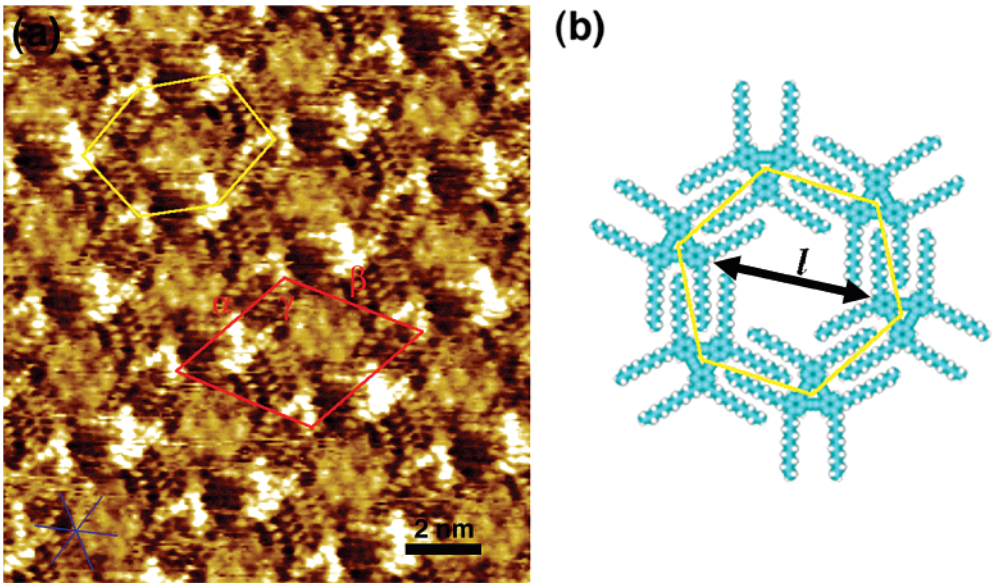

Figure 3. (a) An STM image of **2a** physisorbed at the TCB−HOPG interface. (I_{scl} = 0.50 nA, V_{bias} = −0.99 V). (b) Molecular model of the honeycomb domain of **2a**. The main symmetry axes of graphite are indicated in the lower left corner of the STM image.

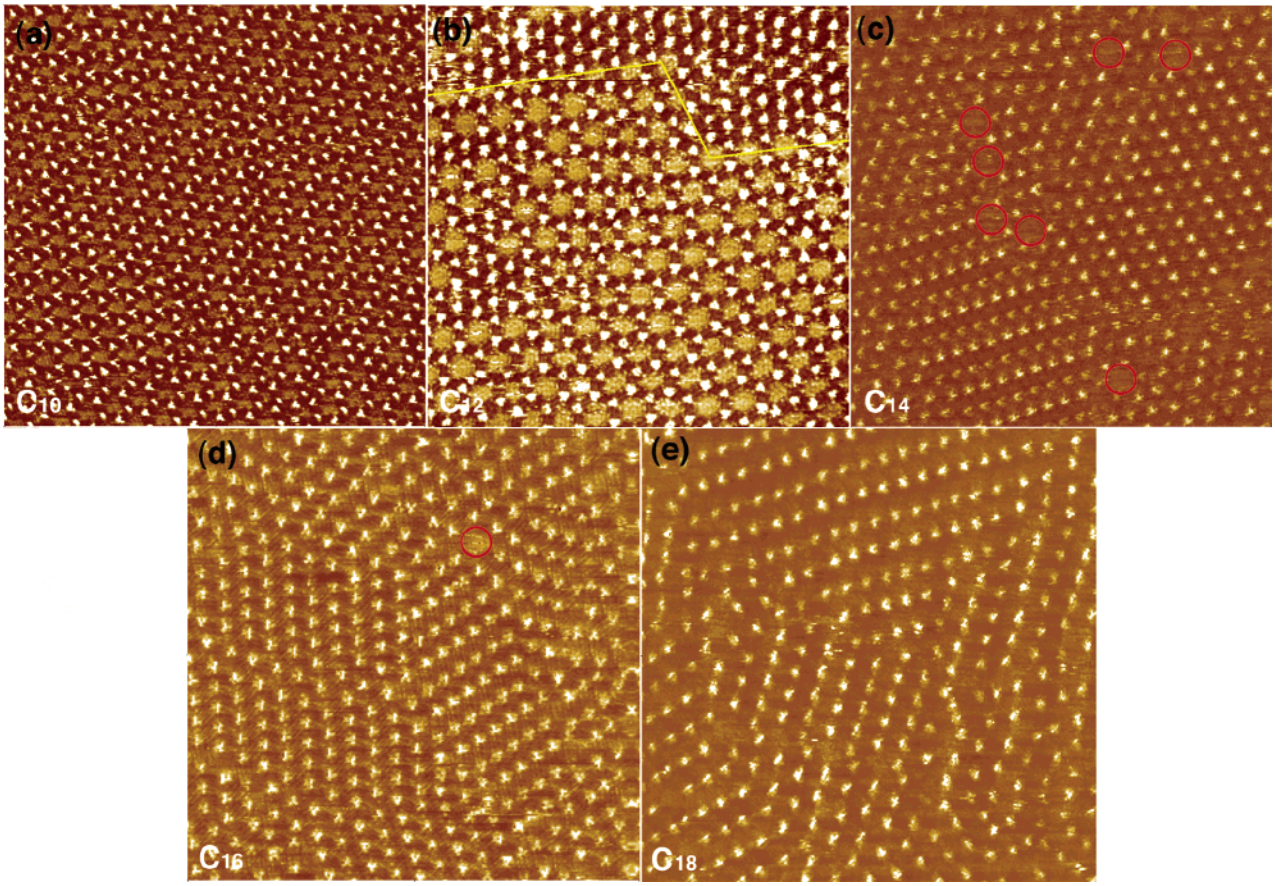

Figure 4. STM images (50 nm × 50 nm) of **3a**−**e** at the TCB−HOPG interface. (a) Honeycomb network of **3a** (I_{scl} = 1.0 nA, V_{bias} = −0.42 V). (b) Honeycomb (bottom) and linear B type (top) networks of **3b** (I_{scl} = 0.60 nA, V_{bias} = −0.28 V). The yellow line separates a honeycomb and a linear B type domain. (c) Linear B type network of **3c** (I_{scl} = 0.65 nA, V_{bias} = −0.18 V). Red circles indicate honeycomb structures observed at domain boundaries. (d) Linear B type network of **3d** (I_{scl} = 0.65 nA, V_{bias} = −0.65 V). A red circle indicates a honeycomb structure. (e) Linear B type network of **3e** (I_{scl} = 0.70 nA, V_{bias} = −0.53 V).

observed. In this system, we observed a dynamic change from a linear structure, called "linear B", which corresponds to the upper domain in Figure 4b to the honeycomb network covering the largest area in this image (See also Figure 5b for a linear B model and Supporting Information). However, a complete conversion to the honeycomb network was within 4 h after dropping a solution onto the HOPG surface never observed. In most cases, a small area of the linear B type packing coexisted

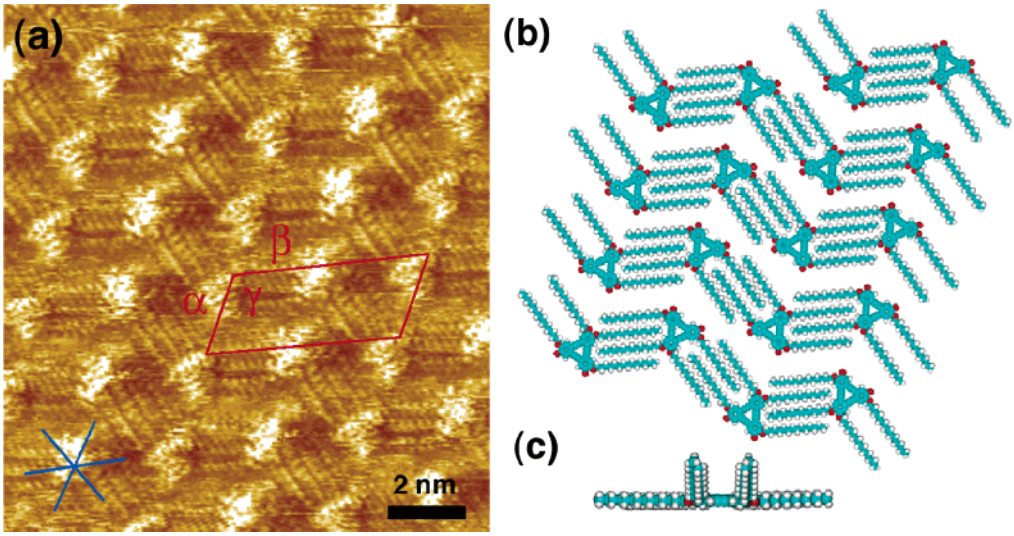

Figure 5. An STM image of a monolayer of **3c** and molecular model of the network at the TCB−graphite interface. (a) Linear B type network (I_{scl} = 0.65 nA, V_{bias} = −0.25 V). Top view (b) and side view (c) of a tentative model representing the linear B type network of **3c**. The main symmetry axes of graphite are indicated in the lower left corner of the STM image.

Table 1. Molecular Networks and Unit Cell Parameters of DBA Derivatives **1a**, **2a**, and **3a**−**e** Physisorbed at the TCB−HOPG Interface

		unit cell parameters[a]				
compound	predominant network	α (nm)	β (nm)	γ (deg)	average APM[b] (nm^2)	NAC[c] on surface
1a	Linear A	2.4 (0.1	2.6 ± 0.1	101 ± 4	6.1	6
	Kagomé	5.0 ± 0.1	4.9 ± 0.1	120 ± 1	7.1	6
2a	Honeycomb	3.9 ± 0.1	3.8 ± 0.2	119 ± 1	6.5	6
3a	Honeycomb	4.2 ± 0.1	3.9 ± 0.1	122 ± 1	6.9	6
3b	Honeycomb[d]	4.5 ± 0.1	4.5 ± 0.1	119 ± 1	8.9	6
3c	Linear B[d]	2.4 ± 0.1	5.4 ± 0.1	112 ± 1	6.0	4
3d	Linear B	2.4 ± 0.1	5.4 ± 0.1	105 ± 2	6.3	4
3e	Linear B[e]	–	–	–	–	–

[a] For each compound, unit cells are indicated in the figures in the main text or in the Supporting Information. [b] Area per molecule. [c] Number of alkyl chains. [d] The linear B and the honeycomb structures occasionally coexist. [e] The cell parameters are not determined due to the low resolution of the STM images.

with the predominant honeycomb network, which is attributed to the elongation of the alkyl chains. Comparison of the unit cell parameters of the honeycomb networks of **2a**, **3a**, and **3b** revealed that the angle (γ) is constant (ca. 120°) while the length of the unit cell vectors α and β increases (from 3.8 to 4.5 nm) upon going from alkyl to alkoxy and increasing the alkoxy chain length (Table 1). Hence, the diameter (l) and area of central void in such a hexagon is controlled by the alkyl chain length (l = 3.1 ± 0.1 nm for **2a**, 3.4 ± 0.2 nm for **3a**, and 3.7 ± 0.2 nm for **3b**).

Molecule **3c** which has six tetradecyloxy chains forms both honeycomb and linear B type domains (Figure 4c). Though large scale images show honeycomb structures near domain boundaries, the linear B network was predominantly observed. No change to the honeycomb structure was observed within 5 h after sample preparation. In linear B domains, molecules have the same orientation in a given row while this orientation alternates from row to row leading to a zigzag alignment. A high-resolution image of **3c** emphasizes the orientation of the alkyl chains (Figure 5a). Four interdigitated alkyl chains between cores are clearly observed. However, the other alkyl chains are not observed presumably because they are not adsorbed on the graphite surface but are exposed to the liquid phase (Figures 5b and 5c).

Upon increasing the alkoxy chain length further (**3d** and **3e**), the same type of linear networks are also predominantly observed (Figures 4d and 4e). The length of the unit cell vectors α and β are similar for **3c** and **3d** (2.4 and 5.4 nm, respectively); however, the angle (γ) of **3d** (105°) is smaller than that of **3c** (112°) (Table 1). In case of **3e**, more randomly ordered areas are observed (Figure 4e).

2.2. Solvent Effect on Molecular Networks of DBAs. (a) Molecular Network of Rhombus-Shaped 1a. The solvent effect on the structure of molecular DBA networks has been examined by comparing their self-assembly in three different organic solvents (1-phenyloctane, *n*-tetradecane, and 1-octanoic acid) in addition to TCB described above. The DBA networks are strongly solvent dependent. As mentioned above, in TCB the linear A network is kinetically favored while the Kagomé network is the thermodynamic stable one. Interestingly, another type of linear structure (linear A′) appeared by changing the solvent. The difference between the linear A and A′ structure is the number of adsorbed alkyl chains on the surface and the density of the molecular networks as described below.

In phenyloctane, the coexistence of Kagomé and linear A′ structures was observed (Figure 6a). The structural details of the linear A′ packing are discussed later.

Figure 6b shows an STM image of a monolayer of **1a** physisorbed from tetradecane on HOPG. In this solvent, small domains of the linear A structure were observed. The network type was confirmed by comparison of the unit cell parameters (α = 2.4 ± 0.1 nm, β = 2.6 ± 0.1 nm, γ = 97 ± 3°) with

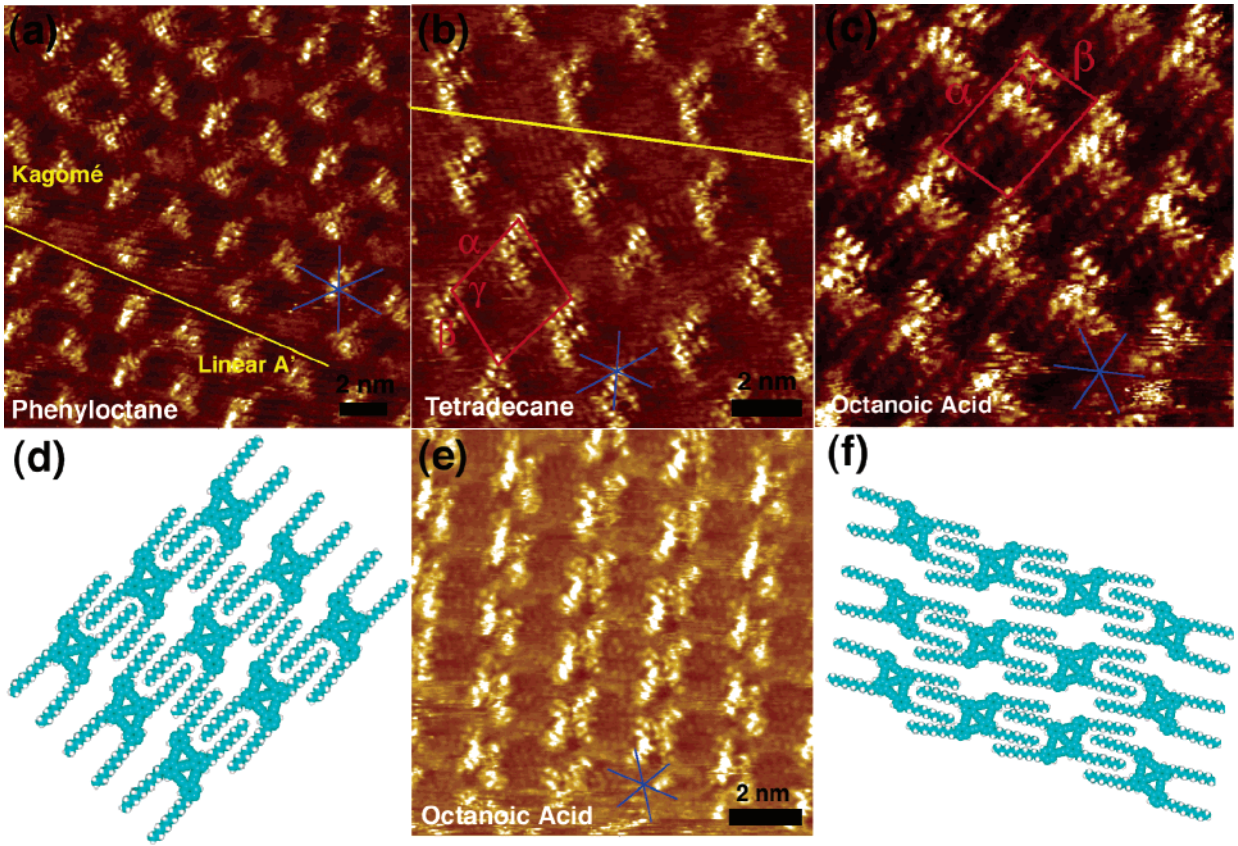

Figure 6. (a) Coexistence of Kagomé and the linear A′ domains of **1a** physisorbed from phenyloctane on HOPG (I_{scl} = 0.70 nA, V_{bias} = −0.54 V). The yellow line separates a Kagomé and a linear A′ domain. (b) Linear A domains of **1a** physisorbed from tetradecane on HOPG (I_{scl} = 0.70 nA, V_{bias} = −0.65 V). Unit cell parameters: $\alpha = 2.4 \pm 0.1$ nm, $\beta = 2.6 \pm 0.1$ nm, $\gamma = 97 \pm 3°$. The yellow line indicates a domain boundary. (c) A high-resolution STM image of the linear A′ type pattern formed upon physisorption of **1a** from octanoic acid (I_{scl} = 0.60 nA, V_{bias} = −0.34 V). All molecules have the same orientation. Unit cell parameters; $\alpha = 2.5 \pm 0.1$ nm, $\beta = 1.9 \pm 0.2$ nm, $\gamma = 100 \pm 2°$. (d) Molecular model of the linear A′ pattern based on the STM image in Figure 6c. (e) Another Linear A′ domain as the result of physisorption of **1a** from octanoic acid on HOPG (I_{scl} = 0.60 nA, V_{bias} = −0.88 V). The difference in the orientation of the molecules in adjacent rows is highlighted. This leads to slightly different unit cell parameters for nonequivalent rows. (f) Molecular model of the linear A′ structure based on the STM image in Figure 6e. The main symmetry axes of graphite are also indicated in the STM images.

those observed for the linear A type in TCB ($\alpha = 2.4 \pm 0.1$ nm, $\beta = 2.6 \pm 0.1$ nm, $\gamma = 101 \pm 4°$). In tetradecane, the Kagomé domain was not observed.

In octanoic acid, bisDBA **1a** dominantly forms the linear A′ structure (Figures 6c and 6e) with sometimes a small Kagomé domain (see Supporting Information). Normally, the conjugated cores are oriented identically throughout a domain (Figure 6c). The corresponding molecular model is shown in Figure 6d. The unit cell parameters are $\alpha = 2.5 \pm 0.1$ nm, $\beta = 1.9 \pm 0.2$ nm, and $\gamma = 100 \pm 2°$. Sometimes, however, the orientation of the conjugated cores in adjacent rows is different as shown in Figure 6e and the molecular model in Figure 6f. The same structural variation is also observed in the linear A′ type domains for monolayers physisorbed from phenyloctane (Figure 6a). However, the overall effect on the monolayer structure is minor (slight difference in the unit cell parameters for nonequivalent rows): the main aspect of the linear A′ pattern is that four alkyl chains per molecule are adsorbed and the monolayer is stabilized by alkyl chain interdigitation.

In both linear A and A′ networks, adjacent cores are connected via four interdigitating alkyl chains. In the linear A structure, the two remaining alkyl chains are adsorbed on the graphite surface, parallel to one of its symmetry axes, while those two alkyl chains in the linear A′ structure are desorbed.

(b) Molecular Network of Triangular-Shaped DBA 2a. For the decyl-substituted triangular compound **2a**, the monolayers show a more complex solvent dependence. Upon physisorption from phenyloctane, dynamic changes in the monolayer structure are observed. Soon after applying a drop on the substrate the trimer structure, which is identical to the network observed in octanoic acid (Figure 7e), appeared. The detailed structure of the trimer network is discussed further in the text. This trimer molecular network gradually transformed into a zigzag alignment (Figures 7a and 7b) and honeycomb structure. Most of trimer domains disappeared within an hour. A zigzag row is indicated in Figure 7a by the yellow line. Triangle-shaped bright features correspond to the π-conjugated cores of DBA. At two sides a core is linked to the adjacent ones by interdigitating alkyl chains. At the third side, two alkyl chains are located between the zigzag rows. Surprisingly, one phenyloctane molecule is coadsorbed between these two non-interdigitated alkyl chains (Figure 7b). This was confirmed by the observation of small bright features that matched the size of the phenyl ring of phenyloctane (see also model in Figure 7c). Unit cell parameters are $\alpha = 3.6 \pm 0.2$ nm, $\beta = 5.0 \pm 0.2$ nm, and $\gamma = 135 \pm 1°$. There are two DBA molecules and two phenyloctane molecules in a unit cell. Moreover, this structure gradually changed to the honeycomb network, resulting in the coexistence of honeycomb and zigzag networks. The formation of the

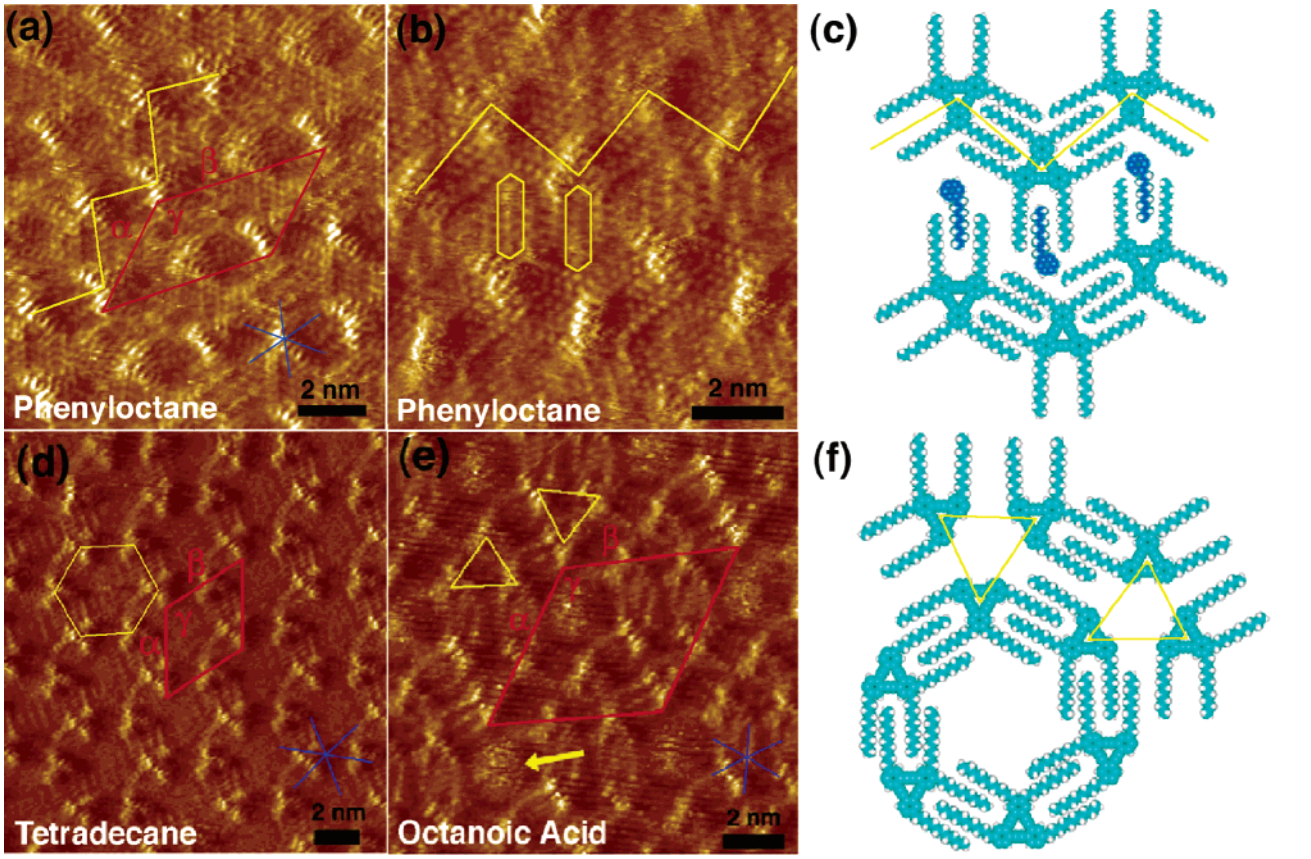

Figure 7. (a) An STM image of a monolayer of **2a** physisorbed from phenyloctane (I_{scl} = 0.85 nA, V_{bias} = −0.133 V). Unit cell parameters; α = 3.6 ± 0.2 nm, β = 5.0 ± 0.2 nm, γ = 135 ± 1°. The yellow line indicates a zigzag row. (b) An STM image of a **2a** pattern formed upon physisorption from phenyloctane (I_{scl} = 1.0 nA, V_{bias} = −0.59 V). Yellow "boxes" indicate coadsorbed phenyloctane molecules. The yellow line marks a zigzag row. (c) Molecular model structure of the zigzag network observed in phenyloctane. (d) An STM image of **2a** physisorbed from tetradecane (I_{scl} = 1.0 nA, V_{bias} = −0.78 V). Unit cell parameters; α = 4.0 ± 0.2 nm, β = 4.0 ± 0.1 nm, γ = 122 ± 2°. (e) An STM image of **2a** in octanoic acid (I_{scl} = 0.90 nA, V_{bias} = −0.66 V). Unit cell parameters; α = 5.9 ± 0.2 nm, β = 5.7 ± 0.2 nm, γ = 122 ± 1°. (f) Tentative model of the trimer network of **2a** in octanoic acid. The yellow arrow indicates a molecule in the center of the hexagon. The main symmetry axes of graphite are also indicated in the lower right part of the STM images.

thermodynamically favored honeycomb network requires the expulsion of coadsorbed phenyloctane molecules and interdigitation of all alkyl chains. Thus, coadsorption of the solvent molecules first led to the formation of the zigzag network from the kinetically favorable trimer structure. Consequently, desorption of the coadsorbed solvent molecules led to the honeycomb network. In spite of the similar alkyl chain length of phenyloctane and octanoic acid, the latter one was not coadsorbed presumably because of homodimer formation involving hydrogen bonding.[27]

Figure 7d shows the honeycomb network of **2a** formed upon self-assembly at the tetradecane−HOPG interface. There is no clear difference between the honeycomb networks observed in TCB and those formed in tetradecane as indicated by their respective unit cell parameters (α = 4.0 ± 0.2 nm, β = 4.0 ± 0.1 nm, γ = 122 ± 2° for tetradecane and α = 3.9 ± 0.1 nm, β = 3.8 ± 0.2 nm, γ = 120 ± 1° for TCB).

Figure 7e is a typical STM image of an adlayer of **2a** on graphite physisorbed from octanoic acid. Three triangular bright features, the π-conjugated cores, form triangular-shaped trimers, as indicated in yellow in Figure 7e. Figure 7f shows a tentative model. Though four alkyl chains per molecule are clearly visible, the other two alkyl chains facing the center of the trimer could not be resolved, suggesting they are too mobile or directed to the liquid phase. Due to the limited degree of alkyl chain interdigitation, molecule−molecule interactions in the trimer networks are expected to be weaker compared to those stabilizing the honeycomb network. Fuzzy spots were observed at the center of the hexagons (Figure 7e, yellow arrow), indicating the adsorption of another **2a** molecule. This structure did not change to other structures even after 5 h at 20−22 °C.

(c) Molecular Networks of Decyloxy-Substituted Triangular DBA 3a. In contrast to decyl-substituted **2a**, compound **3a** forms a hexagonal-like structure in three solvents (phenyloctane, tetradecane, and octanoic acid). Figure 8b represents a typical STM image of **3a** physisorbed from tetradecane on HOPG, revealing the formation of a hexagonal packing. Basically, this hexagonal packing reflects the structure of a honeycomb network and one molecule of **3a** in each central void of the honeycomb. These structural features were confirmed by the observation of the ordering of the alkyl chains. The central molecules in the hexagons appear fuzzy most probably due to their dynamics. In a large hexagonal domain, the adsorption−desorption process of the central molecules was indeed observed in a series of STM of the same area images recorded sequentially (see Supporting Information). The hexagonal structures filled with fuzzy molecular images in the center

(27) (a) Loveluck, G. *J. Phys. Chem.* **1960**, *64*, 385−387. (b) Czarnecki, M. A. *Chem. Phys. Lett.* **2003**, *368*, 115−120. (c) Eliason, T. L.; Havey, D. K.; Vaida, V. *Chem. Phys. Lett.* **2005**, *402*, 239−244.

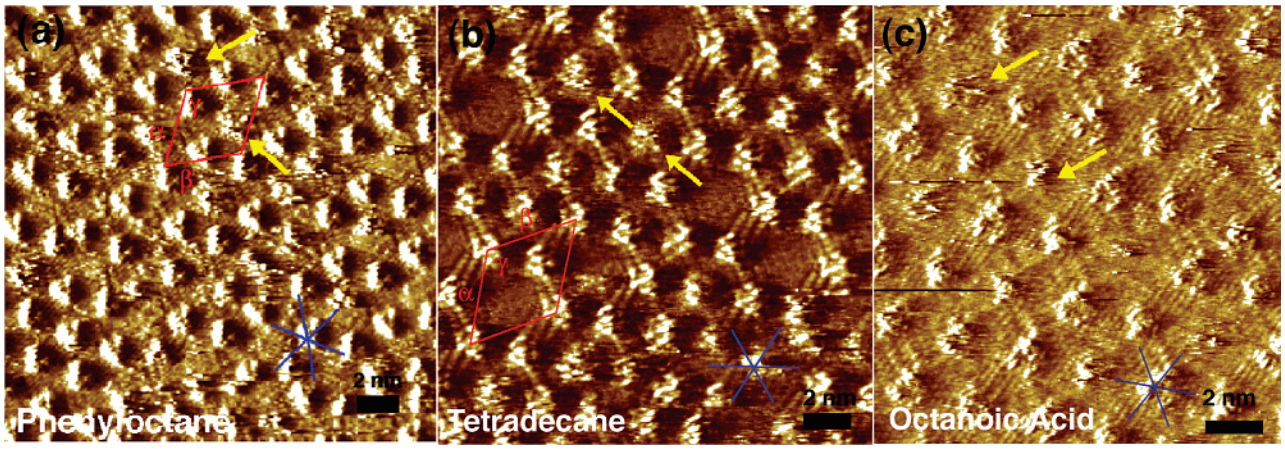

Figure 8. STM images of **3a** physisorbed at the liquid−HOPG interface. The yellow arrows points to molecules at the center of a hexagon. (a) A hexagonal domain of **3a** physisorbed from phenyloctane (I_{scl} = 0.65 nA, V_{bias} = −0.55 V). Unit cell parameters; α = 4.2 ± 0.1 nm, β = 4.1 ± 0.1 nm, γ = 114 ± 1°. (b) A hexagonal domain of **3a** physisorbed from tetradecane (I_{scl} = 0.60 nA, V_{bias} = −0.93 V). Unit cell parameters; α = 4.1 ± 0.2 nm, β = 4.1 ± 0.1 nm, γ = 121 ± 2°. (c) A hexagonal domain of **3a** physisorbed from octanoic acid (I_{scl} = 0.75 nA, V_{bias} = −0.60 V). The main symmetry axes of graphite are also indicated in the STM images.

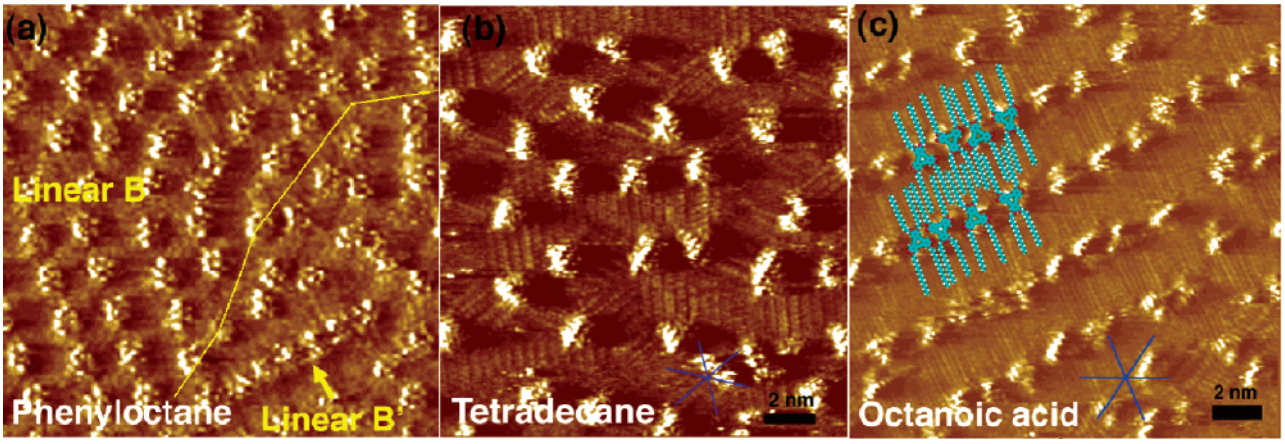

Figure 9. STM images and a tentative packing model of **3d** at the liquid−HOPG interface. (a) Coexistence of the linear B and linear B′ structures upon physisorption of **3d** from phenyloctane (50 nm × 50 nm, I_{scl} = 0.80 nA, V_{bias} = −0.81 V). (b) A random structure in tetradecane (I_{scl} = 0.90 nA, V_{bias} = −0.55 V). (c) A linear B′ domain of **3d** at the octanoic acid−graphite interface (I_{scl} = 0.60 nA, V_{bias} = −0.52 V). Molecular model of the linear B′ domain as observed in tetradecane is superimposed. The main symmetry axes of graphite are also indicated in the lower part of the STM images.

of the voids also appear in phenyloctane (Figure 8a) and octanoic acid (Figure 8c).[28] The unit cell parameters are comparable for the honeycomb and hexagonal structures (α = 4.2 ± 0.1 nm, β = 3.9 ± 0.1 nm, γ = 122 ± 1° for TCB (honeycomb), α = 4.1 ± 0.2 nm, β = 4.1 ± 0.1 nm, γ = 121 ± 2° for tetradecane (hexagonal), and α = 4.2 ± 0.1 nm, β = 4.1 ± 0.1 nm, γ = 114 ± 1° for phenyloctane (hexagonal)).

(d) Molecular Networks of Hexadecyloxy-Substituted Triangular DBA 3d. Solvent-induced changes of the network structure were also observed for **3d**. As described above, at the TCB−HOPG interface, the linear B structure was observed (Figure 4d). After dropping a phenyloctane solution of **3d** on HOPG, the coexistence of the linear B network and a different linear structure (linear B′) was observed (Figure 9a, see Supporting Information). The linear B′ structure was dominantly observed in octanoic acid. The structural details of the linear B′ structure are discussed later. In tetradecane, monolayers become more complex: random structures together with small linear B′ domains are observed (Figure 9b).

Figure 9c shows a typical linear B′ structure with a small random domain of **3d** formed at the octanoic acid−graphite interface. The linear B′ structure consists of molecular rows with an alternating orientation of the molecules in a given row. The intermolecular distance between adjacent molecules in a row is not very well defined but varies slightly. Four alkyl chains per molecule take part in the alkyl chain interdigitation between adjacent rows. The position of the other two alkyl chains could not be determined presumably due to the free movement of the alkyl chains in the solution or because of their mobility on the graphite surface (Figure 9c). All visualized alkyl chains in a given domain lie parallel to one of the three main symmetry axes of graphite.

(28) In phenyloctane, small part of the zigzag structure of **3a** was also observed.

Discussion

Figure 10 summarizes the different types of molecular networks of DBAs **1a**, **2a**, **3a**, and **3d** and their model structures. Rhombic bisDBA **1a** shows three different structures (Figure 10b): Kagomé, linear A, and linear A′. Also decyl-substituted triangular DBA **2a** forms three different networks (Figure 10c): honeycomb, zigzag, and trimer. The alkoxy-substituted triangular DBAs **3a**−**e** show four different structures (Figures 10c, 10d, and 10e): the honeycomb, hexagonal (honeycomb void filled (not shown)), linear B, and linear B′ structures. Also the solubility of the compounds in the different solvents is

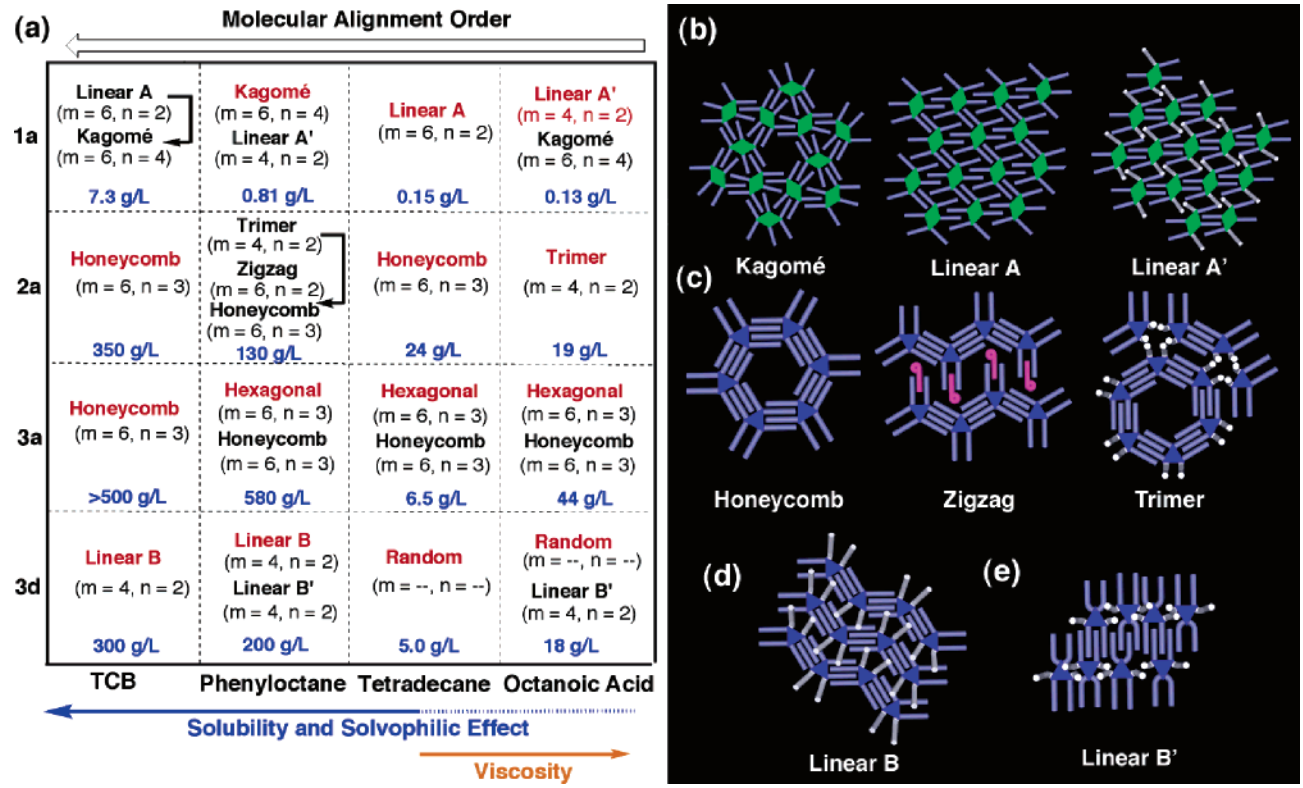

Figure 10. (a) Schematic representation of the different types of interfacial monolayer structures of DBAs **1a**, **2a**, **3a**, and **3d** along with the properties of the solvents used. The major network type is colored in red. The arrows indicate the dynamic conversions. The index m represents the number of alkyl chains adsorbed per molecule on the graphite surface. The index n refers to the number of alkyl chain interdigitation sites per molecule. '*m*' and 'NAC' (Table 1) are equivalent. Large values for *m* and *n* indicate a highly ordered molecular alignment. Solubilities of the compounds in each solvent (g/L) are indicated in blue (refers to the amount of compound dissolved after 12 h at room temperature). (b) Models of the three network structures of **1a** (Kagomé, linear A, and linear A′). (c) Models of the three network structures of DBA **2a** (honeycomb, zigzag, and trimer). (d) A model of the linear B structure of **3d**. (e) A model of the linear B′ structure of **3d**. The brighter rods indicate alkyl chains which are not adsorbed on the surface.

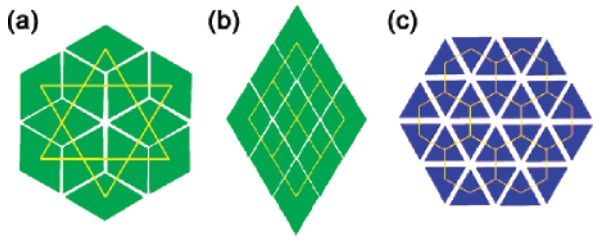

Figure 11. Close packing of rhombi (green) (a, b) and triangles (blue) (c). Connecting the gravity centers of adjacent rhombi or triangles (shown as yellow lines) gives rise to the formation of the Kagomé network in case of rhombi (a) and the honeycomb network in case of triangles (c).

indicated (see also Supporting Information). Here we also introduce indices *m* and *n* which refer to molecule−substrate and molecule−molecule interactions, respectively. The index *m* represents the number of alkyl chains adsorbed per molecule on the graphite surface. The index *n* refers to the number of alkyl chain interdigitation sites per molecule.

1. Core Shape-Directed Kagomé and Honeycomb Network Formation Involving Directional Alkyl Chain Interdigitation. The shape of the π-electron-conjugated systems is one of the important factors which determines the alignment of the DBA molecules on the surface.[16] Interestingly, the observed direction of each π-electron-conjugated system in 2D DBA networks corresponds very well to the ideal dense packing model of rhombi and triangles. Figure 11 shows the "ideal" dense packing mode of rhombi (Figures 11a and 11b) and triangles (Figure 11c).[29] The dense packing models show that all sides of the rhombi and triangles are shared with their neighbors. It should be pointed out that in the networks formed from TCB (the Kagomé network of **1a** and the honeycomb network of **2a**), all sides of the rhombic or triangular π-electron systems in the Kagomé and honeycomb networks are shared with their neighbors via directional alkyl chain interdigitation (Figures 2d and 3b). The linear type alignment of rhombi (Figure 11b), i.e., the linear A structure, is not the thermodynamically most stable structure as the degree of directional alkyl chain interdigitation is lower compared to the Kagomé structure (The details will be discussed in the next section). The shape of the π-electron system thus determines the directional interaction based upon full alkyl chain interdigitation, giving rise to two different structures, the Kagomé (for the rhombic π-electron systems) and the honeycomb (for the triangular π-electron systems).

There are some reports, mainly involving alkoxylated aromatic compounds, on 2D patterns formed as the result of alkyl chain interdigitation as main intermolecular interaction.[30] However, the question arises why both DBAs form regular patterns via directional alkyl chain interdigitation. This question can be answered by comparison of molecular networks of triangle-

(29) The dense packing models of the rhombi and triangle shown in Figure 11 highlight the difference of the positions of the directional interacting sites. These models are not related with the surface coverage of the whole molecular network, i.e., the principle of closest packing, as discussed later.

(30) (a) Qiu, X.; Wang, C.; Zeng, Q.; Xu, B.; Yin, S.; Wang, H.; Xu, S.; Bai, C. L. *J. Am. Chem. Soc.* **2000**, *122*, 5550−5556. (b) Merz, L.; Güntherodt, H.-J.; Scherer, L. J.; Constable, E. C.; Housecroft, C. E.; Neuburger, M.; Hermann, B. A. *Chem. Eur. J.* **2005**, *11*, 2307−2318. (c) Xu, S.; Zeng, Q.; Lu, J.; Wang, C.; Wan, L.; Bai, C. L. *Surf. Sci.* **2003**, *538*, L451−L459.

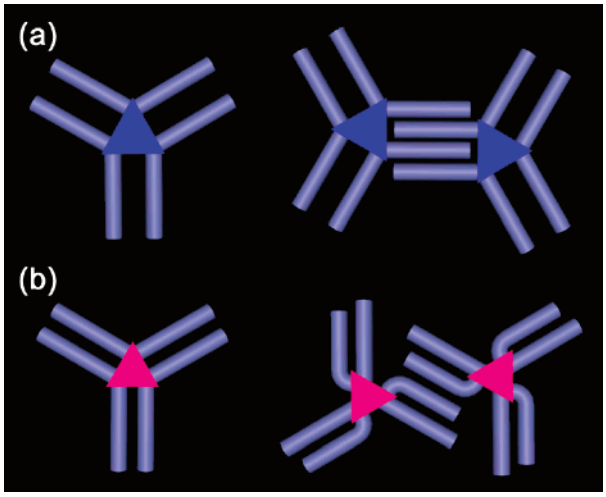

Figure 12. Schematic drawings of the effect of core size on alkyl chain interactions and interdigitation. (a) Triangles with a suitable core size for directional alkyl chain interdigitation with a partner. (b) The core size is too small for directional alkyl chain interdigitation. A side-by-side alignment of alkyl chains is observed.

shaped triphenylene derivatives with those of DBAs **3a**−**e** having the same number and length of alkoxy chains.[31] For example, it has been reported by Bai et al. that triphenylene derivative **4a** with decyloxy side chains shows a hexagonal packing pattern.[31] However, there is a clear difference between the packing patterns of the corresponding DBA **3a** (Figure 3b) and the triphenylene derivative **4a**. Even though the hexagonal network of triphenylene **4a** involves alkyl chain interactions between neighboring molecules, no interdigitation of the alkyl chains is observed because of the small core size. In fact, the closest interatomic distance between two alkoxy oxygen atoms estimated from the optimized geometries of the two model compounds (**3f** and **4b**, R = OMe: obtained by DFT calculations at the B3LYP/6-31g* level of theory) is 0.98 and 0.73 nm, for the annulene and triphenylene, respectively (Figure 1).[32] Moreover, this interatomic distance (0.98 nm) for DBA **3a** relates well with the typical distance between closely packed alkyl chains (0.40−0.45 nm).[33] Therefore, DBA **2a** can interact with adjacent molecules via directional alkyl chain interdigitation (Figure 12a), while triphenylene **4a** cannot accommodate alkyl chains of neighboring molecules between its own alkyl chains (Figure 12b). Alkyl chain interdigitation leads to enhanced molecule−molecule interactions.

Hence, core symmetry, size, and location and orientation of alkyl or alkoxy groups at the periphery of π-electron-conjugated systems are key factors to determine network structure.

2. Dynamic Changes Driven by the Molecule−Molecule Interactions in the Network Formation of 1a in TCB. Molecules generally prefer to pack as densely as possible to maximize the substrate coverage, which is favored for enthalpic reasons (i.e., the principle of closest packing).[15d] We used the average area per molecule on the surface to compare the substrate coverage of the molecules. For different networks consisting of the same molecules, the density of the molecular network can be estimated by comparison of the average area per molecule. The smaller the value of the average area per molecules, the higher the density of the molecular network is and vice versa.

The careful comparison between the linear A structure (Figure 2a) and the Kagomé structure (Figure 2c) disclosed that the dynamic process most likely originates from the difference in molecule−molecule interaction. Because the average area per molecule in the Kagomé structure (7.1 nm^2) is larger than in the linear A structure (6.1 nm^2), we can rule out that in this particular case the surface coverage plays a critical role in defining the network structure. In addition, molecular modeling confirmed that the orientation and conformation of the alkyl chains of **1a** are similar in both the linear A (Figure 2b) and the Kagomé (Figure 2d) networks. Moreover, molecule−substrate and molecule−solvent interactions are similar for both networks. On the other hand, there is a clear difference between both network structures in terms of molecule−molecule interactions (index n in Figure 10). The molecule−molecule interactions are believed to be stronger in the Kagomé structure than in the linear A structure as only in the Kagomé structure the alkyl chains are fully interdigitated ($n = 4$ for the Kagomé network and $n = 2$ for the Linear A network). For this reason, in combination with the solvent effect of TCB described later, the linear A structure gradually changed into the Kagomé network which appeared as the thermodynamically favored structure.

3. Effect of Enhancement of Molecule−Substrate Interactions as a Result of Elongation of Alkoxy Chains of Triangular DBAs. Network structures of aromatic compounds with alkyl substituents on graphite are reported to change by changing the alkyl chain length.[30c,31,34] For the 2D networks of triangle-shaped DBA derivatives **3a**−**e** in TCB, the linear B structure gradually becomes predominant with increasing alkyl chain length (from C_{14} on) due to the increase of the van der Waals interactions in terms of molecule−molecule and molecule−substrate interactions as represented schematically in Figure 13. The dynamic behavior and coexistence of the honeycomb and linear B structures observed for **3b** (C_{12}) indicate that both structures have a comparable free energy. For molecules with longer chains than **3b**, more stable linear B type domains were observed. By comparison with the triphenylene derivatives having six alkoxy chains, it appears that the transition from the hexagonal to the linear structures happens at the same chain length (C_{14}).[31a] A further increase in the length of the alkyl chains leads to a gradual misalignment of these alkyl chains with respect to the main symmetry axes of graphite due to an increased interaction. In the case of **3e**, more randomly oriented small domains of the linear type network were observed than for **3c** and **3d** as shown in Figure 4e. Also triphenylenes with longer alkyl chains show the formation of distorted networks.[31a] This is the result of strong molecule−substrate interactions, which restricts the in-plane mobility and the desorption−adsorption dynamic behavior of the molecules.

(31) (a) Wu, P.; Zeng, Q.; Xu, S.; Wang, C.; Yin, S.; Bai, C. L. *ChemPhysChem* **2001**, *12*, 750−754. (b) Charra, F.; Cousty, J. *Phys. Rev. Lett.* **1998**, *80*, 1682−1685.

(32) Optimization of model compounds were performed under D_{2h} symmetrical constrain for **1b** and D_{3h} symmetrical constrain for **2b**, **3f** and **4b**.

(33) (a) McGonigal, G. C.; Bernhardt, R. H.; Thomson, D. J. *Appl. Phys. Lett.* **1990**, *57*, 28−30. (b) Rabe, J. P.; Buchholz, S. *Science* **1991**, *253*, 424−427. (c) Herwig, K. W.; Matthies, B.; Taub, H. *Phys. Rev. Lett.* **1995**, *75*, 3154−3157. (d) Tao, F.; Bernasek, S. L. *J. Am. Chem. Soc.* **2005**, *127*, 12750−12751.

(34) (a) Askadskaya, L.; Boeffel, C.; Rabe, J. P. *Bunsenges. Phys. Chem.* **1993**, *97*, 517−521. (b) Ito, S.; Wehmeier, M.; Brand, J. D.; Kübel, C.; Epsch, R.; Rabe, J. P.; Müllen, K. *Chem. Eur. J.* **2000**, *6*, 4327−4342. (c) Mena-Osteriz, E. *Adv. Mater.* **2002**, *14*, 609−616.

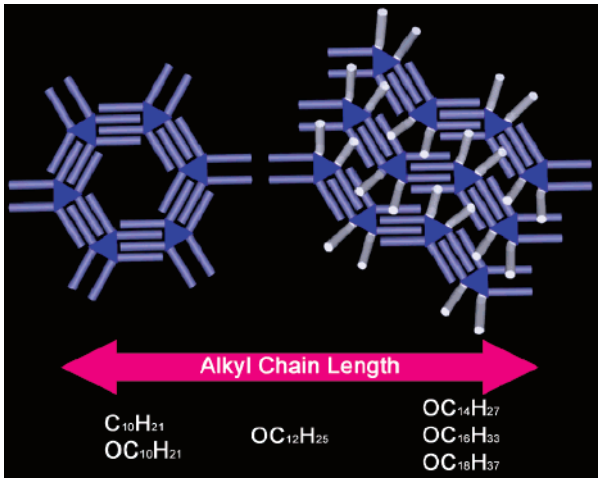

Figure 13. Schematic view of alkyl chain effects in the resulting network structures. The brighter rods indicate alkyl chains which are not adsorbed on the surface.

4. Solvent Effects on the Network Formation of DBA. (a) The Role of the Solvent. Solvent−molecule interactions play an important role in the self-assembly of DBAs. All solvents used (TCB, phenyloctane, octanoic acid,[35] and tetradecane[4b,33a,36]) are known not to form stable monolayers on graphite at room temperature (i.e., weak solvent−substrate interactions). Therefore, the presence of a solvent monolayer can be safely excluded in these solvents. The fact that Kagomé patterns of **1a** and honeycomb domains of **2a** are observed in several structurally noncorrelated solvents indicates that these patterns are not stabilized by the coadsorption of solvent molecules in the network voids. Therefore, we assume that these nanoporous 2D networks are the thermodynamically favored structures.

At the liquid−solid interface, there is an equilibrium between the molecules which stay on the surface (adsorb) and those which go back into the solution (desorb).[15] The overall mobility (in-plane and out-of-plane) of the molecules is important for the transition of the kinetically favored to the thermodynamically favored structure(s). For the in-plane as well as out-of-plane dynamics, the solvents play a significant role. Since the molecules have a solvent-dependent solvation energy, not only the thermodynamic stability of the patterns but also kinetic factors such as the desorption rate and in-plane diffusion rate should be solvent-dependent. In general, for π-electron-conjugated compounds with peripheral alkyl chains, the solvent−molecule interaction can be described in terms of solvophobic and solvophilic effects. These effects have frequently been used to interpret the formation of aggregates of such molecules in solution.[37] Therefore, it seems reasonable to assume that solvophobic effects between DBAs and poor solvents would disfavor or prevent the rearrangement from a kinetically favored pattern to a thermodynamically stable structure. Also it is well documented that the solubility is closely related to the molecule−solvent interaction (solvophilic effect).[38] In addition, the viscosity of the solvent may also affect the out-of-plane (adsorption−desorption dynamics) mobility of the molecules.[15] Higher solvent viscosity would make the rearrangement process slower.

(b) Solvent Effects for the Network Formation of Decyl-Substituted Rhombic 1a and Triangular 2a. Here we discuss the solvent dependence observed for decyl-substituted bisDBA **1a** and DBA **2a**. In aromatic solvents (TCB and phenyloctane), the networks formed by both compounds mainly consist of Kagomé and honeycomb structures, respectively. As a result of strong intermolecular interaction, highly ordered 2D networks are formed. In the aromatic solvents, the thermodynamically stable structures are observed because molecular dynamics should be favored due to the solvophilic effects. Indeed, DBAs **1a** and **2a** are very soluble in TCB and phenyloctane as listed in Figure 10a (**1a**: 7.3 g/L in TCB and 0.81 g/L in phenyloctane, **2a**: 350 g/L in TCB and 130 g/L in phenyloctane). The observed dynamic behavior of **1a** in TCB (transition from the linear A network to the Kagomé network) and **2a** in phenyloctane (from the trimer network via the zigzag network to the honeycomb network) is consistent with this view. In tetradecane, the intermediate case in terms of the solvophilic effect, the properties of the molecular network are somewhat similar to those observed in the aromatic solvents. The linear A structure ($m = 6$, $n = 2$) of **1a** and the honeycomb structure ($m = 6$, $n = 3$) of **2a** were observed. The persistence of the linear A structure in tetradecane may be ascribed to the low mobility of **1a** in this solvent. The intermediate solvophillic effect of tetradecane is also supported by the solubility measurements of **1a** in each solvent as shown in Figure 10a (0.15 g/L in tetradecane). In contrast, in octanoic acid remarkably different network structures, the linear A′ structure ($m = 4$, $n = 2$) of **1a** and the trimer structure ($m = 4$, $n = 2$) of **2a**, were observed. Both networks do not show the maximum possible alkyl chain interdigitation interactions ($n = 2$) and two alkyl chains per molecule do not interact strongly with graphite or are directed to solvent ($m = 4$), leading to a limited stability. As a result, the network density is higher than in aromatic solvents. Indeed, the average area per molecule of **1a** is 7.1 nm^2 for the Kagomé network in TCB and 4.7 nm^2 for the linear A′ network in octanoic acid.[39] For the molecular network of **2a**, the average area per molecule is 6.5 nm^2 for the honeycomb network in TCB and 4.8 nm^2 for the trimer network in octanoic acid. We assume that the rearrangement process of the molecular networks is restricted in octanoic acid because of the low solubility of the DBAs (**1a**: 0.13 g/L, **2a**: 19 g/L). However, there is no significant difference in the solubilizing properties between tetradecane and octanoic acid for both compounds. Though the reason for this significant solvent effect is unclear, one of the possibilities that may lead to the observed differences is the solvent viscosity.[40]

In conclusion, the solvent affects the speed of conversion from a kinetically favored structure to a thermodynamically preferred pattern. The rate of such a rearrangement process is most likely

(35) The desorption energy of the octanoic acid dimer from the graphite surface is lower than that of tetradecane, see: Ref. 10c.

(36) (a) Katsonis, N.; Marchenko, A.; Taillemite, S.; Fichuo, D.; Chouraqui, G.; Aubert, C.; Malacria, M. *Chem. Eur. J.* **2003**, *9*, 2574−2581. (b) Bucher, J. P.; Roeder, H.; Kern, K.; *Surf. Sci.* **1993**, *289*, 370−380. (c) Perronet, K.; Charra, F. *Surf. Sci.* **2004**, *551*, 213−218.

(37) (a) Smithrud, D. B.; Diederich, F. *J. Am. Chem. Soc.* **1990**, *112*, 339−343. (b) Cram, D. J.; Choi, H.-J.; Bryant, J. A.; Knobler, C. B. *J. Am. Chem. Soc.* **1992**, *114*, 7748−7765. (c) Lahiri, S.; Thompson, J. L.; Moore, J. S. *J. Am. Chem. Soc.* **2000**, *122*, 11315−11319. (d) Höger, S.; Bonrad, K.; Mourran, A.; Beginn, U.; Möller, M. *J. Am. Chem. Soc.* **2001**, *123*, 5651−5659. (e) Tobe, Y.; Utsumi, N.; Kawabata, K.; Nagano, A.; Adachi, K.; Araki, S.; Sonoda, M.; Hirose, K.; Naemura, K. *J. Am. Chem. Soc.* **2002**, *124*, 5350−5364. (f) Kastler, M.; Pisula, W.; Wasserfallen, D.; Pakula, T.; Müllen, K. *J. Am. Chem. Soc.* **2005**, *127*, 4286−4296. (g) Terech, P.; Weiss, R. G. *Chem. Rev.* **1997**, *97*, 3133−3160.

(38) (a) Anslyn, E. V.; Dougherty, D. A. *Modern Physical Organic Chemistry*; University Science Books: Sausalito, CA, 2004; pp 153−157. (b) Shinoda, K. *Principles of Solution and Solubility*; Marcel Dekker: New York, 1978.

(39) The addition of the area occupied by two alkyl chain (<1.2 nm^2) to the average area per molecules of the linear A′ increases the area to ca. 5.9 nm^2, which is also smaller than that of the Kagomé network.

dominated by the solubilizing properties of the solvent. Additionally, the viscosity of the solvent can also affect the rearrangement process in the poor solvents. DBAs tend to form a kinetically favored, less ordered structure initially. If the mobility of the DBAs is large enough, the DBA networks will rearrange to more ordered structures despite the fact that the surface coverage is reduced.

(c) Effects of Ether Functionalities. A notable difference in the solvent effect between the molecular ordering of alkyl-substituted **2a** and that of alkoxy-substituted **3a** was observed, though both have the same π-conjugated core and identical alkyl chain lengths. In contrast to **2a** which forms the honeycomb network in TCB and tetradecane, the trimer → zigzag → honeycomb networks in phenyloctane, and the trimer structure in octanoic acid, the alkoxy derivative **3a** forms hexagonal-like networks in all solvents; the honeycomb network in TCB and the hexagonal network in the other solvents. Both networks, so also the hexagonal network, are characterized by the honeycomb alignment as the basic motif. The differences with the alkyl derivatives most likely originate from the conformational flexibility of the ether group located between the aromatic core and the alkyl chains. Indeed, the solubility of **3a** is higher than that of **2a**. Therefore, the network transformations of **3a** might become easier than those of **2a**, and accordingly **3a** forms optimal alkyl chain interdigitation in all solvents. These results suggest that the mobility of the alkyl chains may also affect the molecular mobility thereby affecting the 2D network formation and the outcome of the self-assembly process.

(d) Solvent Effects for the Network Formation of Hexadecyloxy-Substituted Triangular 3d. Hexadecyl-substituted **3d** shows complex patterns upon changing the solvents. In aromatic solvents, the linear B structure is formed. Linear B′ and amorphous like random patterns are observed in tetradecane and octanoic acid. It is expected that the linear B network ($m = 4$, $n = 2$) of **3d** is thermodynamically more preferred than the linear B′ ($m = 4$, $n = 2$) or the random patterns. Even though both networks are characterized by the same index numbers ($m = 4$, $n = 2$), the linear B′ pattern is considered to be the less ordered and less stable one as this packing is strictly spoken not 2D crystalline (slight positional differences of the triangular cores) and the domain sizes are small.

As shown in Figure 10a, the solubility of **3d** in tetradecane and octanoic acid is much lower compared to the solvents containing aromatic groups (5.0 g/L for tetradecane and 18 g/L for octanoic acid). Therefore, lack of favorable solvation interactions and the presence of strong molecule−substrate interactions, due to the long alkyl chains, restrict the dynamic rearrangement process. As a result, kinetically favored though less ordered patterns are observed in poor solvents.

Summary

In summary, we have accomplished STM measurements of a series of DBA derivatives at the liquid−graphite interface. The core symmetry and position of the alkyl or alkoxy chains determine the molecular ordering. In combination with the core size, these structural properties favor the formation of nonpolar porous networks thanks to the directional interdigitation of alkyl chains as well as the registry of the alkyl chains with the main symmetry axes of the substrate. Because of the strong directional alkyl chain interdigitation, 2D open networks with voids are formed. Tuning molecule−substrate interactions, realized for instance by changing the length of the alkyl chains, leads to different molecular networks. Therefore, molecule−molecule and molecule−substrate interactions can be controlled by rational molecular design. The synthetic versatility of DBA derivatives[22,41] will allow us to make various molecular networks with specific topologies. Moreover, the formation of regularly spaced voids in the Kagomé network of bisDBA **1a** and the honeycomb structures of DBAs (**2a**, **3a**, and **3b**) suggests that the central free space can be used as the host space for guest molecules which otherwise would not adsorb on graphite.[7,8]

The solvent plays a significant role in the formation of DBA networks, basically by affecting the number of adsorbed alkyl chains and the degree of alkyl chain interdigitation. In addition to the well-established co-adsorption effects of solvents, the present study highlights other aspects. The solvent-induced polymorphism discloses that perfect molecular networks (maximal directional alkyl chain interdigitation) can be achieved in good aromatic solvents. On the other hand, the molecular network partially loses this stabilizing interaction in poor solvents, resulting in a decrease of network order. These solvent effects on the 2D networks can be attributed to solvophobic/solvophilic interactions between molecules and solvents during the formation of molecular networks. We propose here that the solubilizing properties of the solvents critically change the rate of the rearrangement processes which transform the initially formed kinetically favored structure into the thermodynamically stable final pattern. These insights are useful in the area of "2D crystal engineering."

Acknowledgment. This work was supported by CREST of JST (Japan Science and Technology Agency) and a Grant-in-Aid for Scientific Research from the Ministry of Education, Culture, Sports, Science, and Technology, Japan. S.F. is grateful to the JSPS Postdoctoral Fellowships for Research Abroad. S.D.F. and F.D.S. thank the Federal Science policy through IUAP-V-03, the Institute for the promotion of innovation by Science and Technology in Flanders (IWT), and the Fund for Scientific Research-Flanders (FWO). This paper is dedicated to Professor Philip E. Eaton on the occasion of his 70th birthday.

Supporting Information Available: Synthetic procedures for **3a**−**e**, experimental details, STM images of **1a**, **2a**, and **3a**−**e**, optimized structures of model compounds **1a**, **2b**, **3f**, and **4b**. This material is available free of charge via the Internet at http://pubs.acs.org.

JA0655441

(40) Viscosities of the solvents at 20 °C are 1.41 cP for TCB, 2.58 cP for phenyloctane, 2.33 cP for tetradecane, and 5.83 cP for octanoic acid. (a) Ducoulombier, D.; Zhou, H.; Boned, C. Peyrelasse, J.; Saint-Guirons, H.; Xans, P. *J. Phys. Chem.* **1986**, *90*, 1692−1700. (b) Beilstein, *Handbuch der Organishen Chemie*, 4 Aufl., E IV 5, 1978; p 664. (c) *Techniques of Chemistry, Organic Solvent*; Riddick, J. A., Bunger, W. B., Eds.; Wiley-Interscience: Toronto, 1970; p 261.

(41) (a) Tobe, Y.; Sonoda, M. In *Modern Cyclophane Chemistry*; Gleiter, R., Hopf, H., Eds.; Wiley−VCH: Weinheim, 2004; pp 1−40. (b) Jones, C. S.; O'Connor, M. J.; Haley, M. M. In *Acetylene Chemistry: Chemistry, Biology and Material Science*; Diederich, F., Stang, P. J., Tykwinski, R. R., Eds.; Wiley-VCH: Weinheim, 2005; pp 303−385.